

## Antiviral Prodrugs

Zitierweise: *Angew. Chem. Int. Ed.* **2020**, *59*, 20154–20160

Internationale Ausgabe: doi.org/10.1002/anie.202008665

Deutsche Ausgabe: doi.org/10.1002/ange.202008665

# The Enzyme-Free Release of Nucleotides from Phosphoramidates Depends Strongly on the Amino Acid

Dejana Jovanovic, Peter Tremmel, Pradeep S. Pallan, Martin Egli\* und Clemens Richert\*

**Abstract:** Phosphoramidates composed of an amino acid and a nucleotide analogue are critical metabolites of prodrugs, such as remdesivir. Hydrolysis of the phosphoramidate liberates the nucleotide, which can then be phosphorylated to become the pharmacologically active triphosphate. Enzymatic hydrolysis has been demonstrated, but a spontaneous chemical process may also occur. We measured the rate of enzyme-free hydrolysis for 17 phosphoramidates of ribonucleotides with amino acids or related compounds at pH 7.5. Phosphoramidates of proline hydrolyzed fast, with a half-life time as short as 2.4 h for Pro-AMP in ethylimidazole-containing buffer at 37°C; 45-fold faster than Ala-AMP and 120-fold faster than Phe-AMP. Crystal structures of Gly-AMP, Pro-AMP,  $\beta$ Pro-AMP and Phe-AMP bound to RNase A as crystallization chaperone showed how well the carboxylate is poised to attack the phosphoramidate, helping to explain this reactivity. Our results are significant for the design of new antiviral prodrugs.

## Introduction

Viral respiratory diseases, like COVID-19, call for new antivirals. Among the most important targets for antivirals are polymerases. For positive-strand RNA viruses like hepatitis C virus and SARS-CoV-2, the RNA-dependent RNA polymerase (RdRp) may be inhibited.<sup>[1]</sup> Such RdRp's or replicases represent excellent targets, as the cell does not possess such an RNA-dependent polymerase, so that selectivity may be achieved, and side effects may be minimized. The substrates for RdRp's are ribonucleoside triphosphates (NTPs). Nucleoside-based analogues that compete with the natural substrates and that cause chain termination are known to act as inhibitors.<sup>[2]</sup> Either direct chain termination may be induced, using nucleosides that lack a 3'-hydroxy group, or delayed

termination with non-obligate inhibitors whose sterically demanding substituents shut down extension after further elongation. The latter have the potential to bypass excision by the exonuclease domain of the replication complex.<sup>[3]</sup>

Nucleoside phosphates do not diffuse across cell membranes and lack bioavailability. As a consequence, prodrugs with masked phosphate group have been developed.<sup>[4,5]</sup> One example of this is the ProTide methodology developed by McGuigan in the early 1990s.<sup>[6,7]</sup> ProTides are nucleoside analogues with their phosphate group masked by an *O*-aryl group and an amino acidyl ester moiety *N*-linked to the same phosphate as a phosphoramidate. Due to their increased lipophilicity these compounds are able to penetrate cell membranes.<sup>[4]</sup>

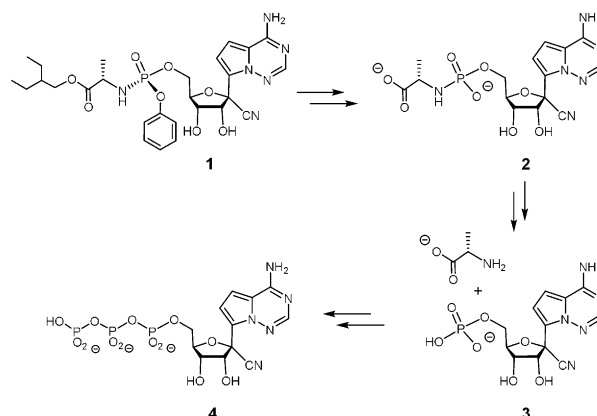
Once inside the cell, the prodrug is converted to the inhibitor triphosphate in a series of metabolic steps. Two FDA approved drugs, sofosbuvir<sup>[8]</sup> and tenofovir alafenamide,<sup>[9]</sup> use this principle, and so does remdesivir, the first antiviral to obtain emergency use authorization for treatment of COVID-19 by the U.S. Food and Drug Administration.<sup>[10,11]</sup>

Both sofosbuvir and remdesivir are phenyl esters of an alkyl amino acidyl phosphoramidate. Because they possess the 5'-phosphate group in protected form, the nucleoside kinase reaction that often limits the activity of nucleoside drugs *in vivo* can be bypassed.<sup>[12]</sup> However, the release of the free monophosphate requires several steps.<sup>[13]</sup> For remdesivir (**1**), formerly known as GS5734<sup>[14]</sup> and originally developed for treatment of Ebola,<sup>[15]</sup> the reaction sequence of Scheme 1 has been proposed.<sup>[15]</sup> It starts with the cleavage of the amino acid ester of **1** by an esterase. The resulting free carboxylate then displaces the aryloxy leaving group by nucleophilic

\*] M. Sc. D. Jovanovic, Dr. P. Tremmel, Prof. C. Richert  
Institut für Organische Chemie, Universität Stuttgart  
70569 Stuttgart (Germany)  
E-Mail: lehrstuhl-2@oc.uni-stuttgart.de  
Dr. P. S. Pallan, Prof. Dr. M. Egli  
Department of Biochemistry  
Vanderbilt University, School of Medicine  
Nashville, TN 37232 (USA)  
E-Mail: martin.egli@vanderbilt.edu

Supporting information and the ORCID identification number(s) for the author(s) of this article can be found under:  
<https://doi.org/10.1002/anie.202008665>.

© 2020 The Authors. Published by Wiley-VCH GmbH. This is an open access article under the terms of the Creative Commons Attribution Non-Commercial License, which permits use, distribution and reproduction in any medium, provided the original work is properly cited, and is not used for commercial purposes.



**Scheme 1.** Conversion of remdesivir (**1**) to the alanine metabolite **2**, followed by hydrolysis to **3** and enzymatic phosphorylation to triphosphate **4**.<sup>[15]</sup> Other ProTides follow similar pathways.

attack on the phosphorus, resulting in a cyclic acyl phosphoramidate (CAPA).<sup>[16]</sup> Spontaneous hydrolysis of this intermediate leads to the phosphoramidate metabolite **2** that may subsequently be cleaved by a histidine triad nucleotide binding (HINT) enzyme<sup>[17,18]</sup> to the nucleoside monophosphate **3**. Subsequent enzymatic phosphorylation steps then give pharmacologically active **4**.

Remdesivir is less well studied than sofosbuvir. Detailed studies on the intracellular metabolism have been published for the latter ProTide. Murakami et al. measured several metabolites over time in hepatocytes and reported that the cleavage of the *P*–*N* bond can be rate limiting.<sup>[19]</sup> Their data indicate that Hint1 is at least partially responsible for the hydrolytic removal of the alanine residue in those cells, but the  $K_m$  values of Hint enzymes for alaninyl phosphoramidates were found to be in the millimolar range.<sup>[19,20]</sup> The same group also found a marked difference in the rates of intracellular conversion among different hepatocyte cell lines. Preclinical work with a 3'-isobutyryl ester also showed strong differences in metabolism and pharmacokinetics between different animal models.<sup>[21]</sup> Tissue pharmacokinetics from a clinical study then revealed that sofosbuvir and its metabolites are accumulated in the liver, with total nucleotide/metabolite levels 30-fold higher than the maximal level in plasma.<sup>[22]</sup> This leaves open the question of what levels metabolites reach in tissues that do not benefit from first pass hepatic extraction and how successful their activation is in cells that are metabolically less active than hepatocytes or tumor cells.<sup>[23]</sup>

The amino acid found in remdesivir and sofosbuvir is L-alanine. Early screens of amino acidyl phosphoramidates of deoxynucleoside analogues with different chain lengths had shown that  $\alpha$ -amino acids are required for good anti-HIV activity<sup>[24]</sup> and that the methyl esters of alanine are among the most potent inhibitors.<sup>[25]</sup> Later in vitro screens against HIV and HSV as well as tumor cells gave similar results.<sup>[13,23]</sup> Alanine is the only amino acid found in ProTide phosphoramidates that have entered the clinic,<sup>[4]</sup> and it is unclear how constructs with other amino acids would perform in vivo. If they were to liberate the free nucleotide in the affected cells without the need for a Hint enzyme, a robust mechanism of action may result, particularly for phosphoramidates with sterically hindered secondary amines, for which Hint1 was reported to have poor activity.<sup>[26]</sup>

There is data that suggests that phosphoramidates with amino acids other than alanine are active antivirals. Herdewijn and colleagues had observed that the asparagine phosphoramidate of dAMP can be a substrate for HIV-1 reverse transcriptase,<sup>[27]</sup> and that aspartic acid-containing nucleotide analogues are active against HCV in vitro.<sup>[28]</sup> When hydrolysis was studied for a series of aminoacyl phosphoramidates at different pD values and temperatures up to 80 °C,<sup>[29]</sup> nucleosides, rather than nucleotides, were observed as main products.<sup>[29]</sup> A preferred cleavage of the phosphoester bond to the nucleoside had also been found in the pH range of 1–3, in early work by Shabarova and colleagues.<sup>[30,31]</sup> Needless to say, dephosphorylation of a nucleotide metabolite through cleavage of the *P*–*O* bond is not desirable for a metabolite of a ProTide prodrug.<sup>[32]</sup> Rather, a preferred cleavage of the *P*–*N* bond, similar to what is found

for reactions catalyzed by human hHint1,<sup>[33]</sup> but without the limitations of substrate specificity and tissue distribution of the enzyme, would be attractive.

In our study on the formation of peptido RNAs from amino acids and ribonucleotides, we had induced the release of 5'-phosphorylated nucleosides and oligomers of phenylalanine from phosphoramidate-linked peptido RNAs with acetic acid in the cold.<sup>[34]</sup> When we studied reactions involving other amino acids quantitatively, we noticed significant hydrolysis of phosphoramidates at neutral pH. This hydrolysis via *P*–*N* bond cleavage was strongly dependent on the structure of the amino acid in an unexpected way. Here we report the rapid enzyme-free release of nucleoside monophosphates from prolinyl phosphoramidates at 37 °C and pH 7.5 in imidazole-containing buffers.

## Results and Discussion

We synthesized the phosphoramidates of Figure 1 to measure the enzyme-free release of ribonucleotides. The group of test compounds included amidates with mono-, di- and tripeptide residues, as well as amidates of related amines lacking a carboxylate. The increasing length of the peptide chains places the carboxy group at different distances from the phosphorus center, where it may attack as a nucleophile. Remdesivir is an analogue of adenosine monophosphate (AMP), and most of the *N*-nucleosides tested are phosphoramidates of AMP, but nucleotides with pyrimidine bases were also included in our study (**12**, **13**). For lipophilic amino acids or peptides, our two-step synthesis employed started with the

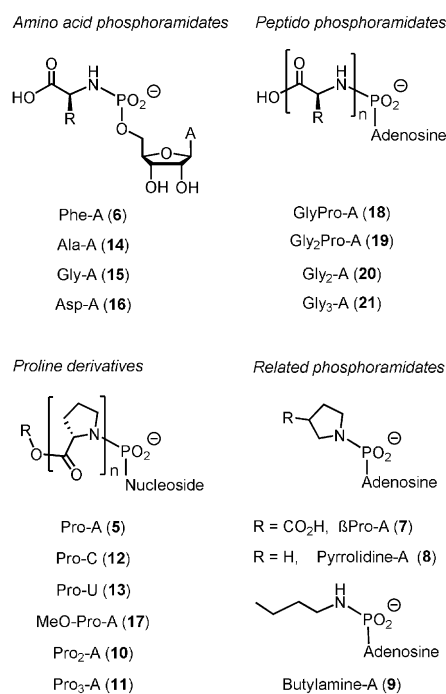


**Figure 1.** Phosphoramidates tested; amino acid residues are given in three-letter code, adenosyl residues are abbreviated as Adenosine in all but the first structure.

preparation of the 2-methylimidazolidine of the nucleotide, which was then reacted with the amine. For more polar amino acids, the methyl ester was coupled to the free ribonucleotides using EDC, followed by purification and a final deprotection step under basic conditions (see the Supporting Information, SI, for details).

We measured the rate of hydrolysis in aqueous HEPES/1-ethylimidazole buffer, pH 7.5, containing 0.08 M MgCl<sub>2</sub> via <sup>31</sup>P NMR. This combination of buffer components has previously been used successfully for the quantitative analysis of the formation of peptido RNAs.<sup>[35,36]</sup> Figure 2 shows spectra and kinetics for the prolinyl phosphoramidate Pro-A (**5**) at 37 °C. Besides free AMP, small quantities of pyrophosphate (PP) and phosphodiester (PD) were formed, as expected at the 10 mM nucleotide concentration employed for NMR monitoring, where intermolecular reactions between nucleo-

tides are more likely than at typical therapeutic concentrations. The hydrolysis itself followed pseudo-first order kinetics. Monoexponential fits to the data points gave the apparent rate constants and half-life times listed in Table 1.

When the first screen, performed at 0 °C as in our earlier work on peptido RNAs,<sup>[34–36]</sup> gave unexpected differences in the rate of hydrolysis of amidates (entries 1–7), we decided to measure a larger data set at physiological temperature (37 °C). Again, the effect of the amino acid structure on the liberation of the nucleotide was strong. At either temperature, proline phosphoramidates released the nucleoside monophosphate much faster than the amidates of other amino acids. At body temperature, the half-life time (*t*<sub>1/2</sub>) of Pro-A was just 2.4 h in our buffer. The pyrimidine nucleotides Pro-C and Pro-U also gave half-life times below 5 h. The alanine phosphoramidate Ala-A found in remdesivir and sofosbuvir hydrolyzes approx. 45-fold more slowly than Pro-A. The rate of hydrolysis of Gly-A and Asp-A was similar to that of Ala-A, whereas Phe-A hydrolyzed more slowly still, with a half-life time 120-fold longer than that of Pro-A. Detailed data for the kinetics measured can be found in the Supporting Information (Figures S35–S86).

Magnesium ions are not required for rapid hydrolysis, as evidenced by the slightly accelerated rate in the absence of

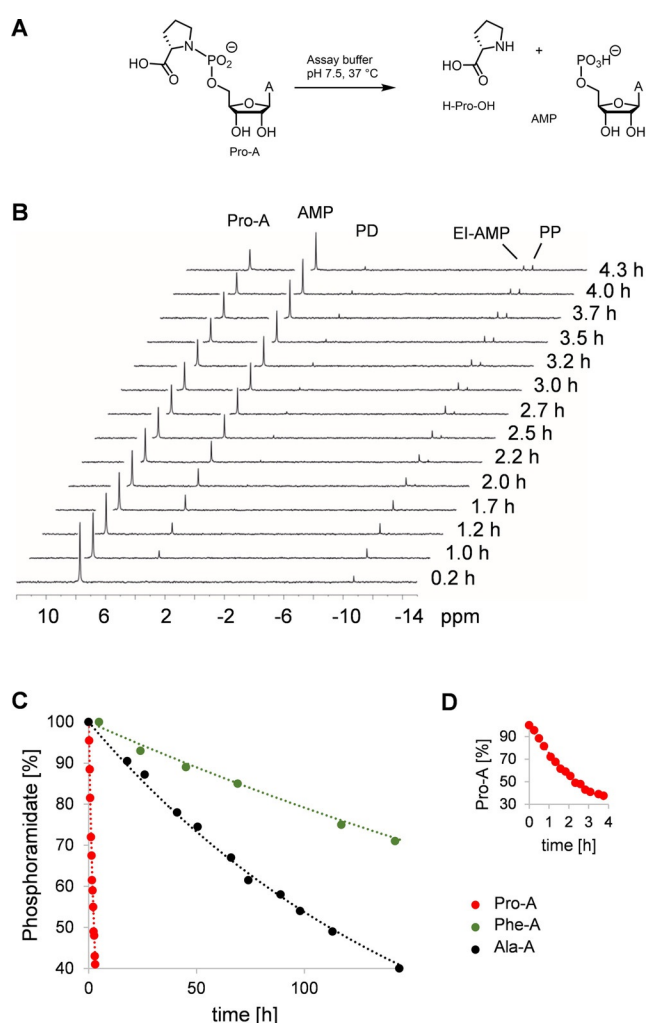


**Figure 2.** Hydrolysis of phosphoramidates. A) Reaction scheme for the proline amidate Pro-A (**5**). B) Overlay of <sup>31</sup>P NMR spectra with signals for Pro-A, AMP, symmetrical pyrophosphate (PP), ethylimidazolium phosphate (EI-AMP) and phosphodiester (PD) labeled.<sup>[36]</sup> C) Comparison of the kinetics of hydrolysis for Pro-A (**5**), Ala-A (**14**) and Phe-A (**6**); broken lines are monoexponential fits. D) Expansion of the kinetics for Pro-A for the first 4 h. Conditions: 37 °C, 10 mM phosphoramidate, 0.5 M HEPES, 0.15 M 1-ethylimidazole, 0.08 M MgCl<sub>2</sub>, pH 7.5.

**Table 1:** Rate constants and half-life times of hydrolysis of phosphoramidates in enzyme-free buffer, pH 7.5 at 0 or 37 °C.<sup>[a]</sup>

Entry No.	Phosphoramidate	Rate constant [h <sup>-1</sup> ]	Half-life <sup>[b]</sup> [days]
<i>T</i> = 0 °C			
1	Pro-A	4.7 × 10 <sup>-3</sup>	6.1
2	Phe-A	5.2 × 10 <sup>-5</sup>	693
3	βPro-A	1.8 × 10 <sup>-3</sup>	14.4
4	Pyrr-A	9.9 × 10 <sup>-4</sup>	28.9
5	BuNH-A	1.9 × 10 <sup>-4</sup>	139
6	Pro <sub>2</sub> -A	1.7 × 10 <sup>-3</sup>	17.0
7	Pro <sub>3</sub> -A	4.8 × 10 <sup>-4</sup>	63.0
<i>T</i> = 37 °C			
8	Pro-A	0.28	0.10
9	Pro-C	0.23	0.13
10	Pro-U	0.17	0.17
11	Pro-A (-Mg <sup>2+</sup> ) <sup>[c]</sup>	0.32	0.07
12	Pro-A (His) <sup>[d]</sup>	6.9 × 10 <sup>-2</sup>	0.41
13	Pro-A (Melm) <sup>[e]</sup>	2.9 × 10 <sup>-2</sup>	0.96
14	Ala-A	6.2 × 10 <sup>-3</sup>	4.68
15	Gly-A	7.7 × 10 <sup>-3</sup>	3.76
16	Asp-A	6.2 × 10 <sup>-3</sup>	4.62
17	Phe-A	2.3 × 10 <sup>-3</sup>	12.4
18	MeO-Pro-A	8.4 × 10 <sup>-3</sup>	3.61
19	Pyrr-A	0.09	0.33
20	BuNH-A	1.1 × 10 <sup>-2</sup>	2.60
21	Pro <sub>3</sub> -A	0.15	0.19
22	GlyPro-A	2.4 × 10 <sup>-3</sup>	12.0
23	Gly <sub>2</sub> Pro-A	1.0 × 10 <sup>-3</sup>	26.6
24	Gly <sub>2</sub> -A	9.2 × 10 <sup>-4</sup>	33.0
25	Gly <sub>3</sub> -A	5.8 × 10 <sup>-4</sup>	49.5

[a] Conditions: 0.50 M HEPES or MOPS, no or 0.08 M MgCl<sub>2</sub>, 0.15 M buffer additive (1-ethylimidazole) and pH 7.5, see SI for details.

[b] Pseudo-first order rate constant obtained by monoexponential fit.

[c] Buffer without MgCl<sub>2</sub>. [d] Buffer with histidine instead of 1-ethyl-

imidazole. [e] Buffer with 2-methylimidazole instead of 1-ethylimidazole.

the divalent cation (entry 11, Table 1). The imidazole component has a strong effect, though, with a significant change in rate when 1-ethylimidazole was replaced with imidazole or 2-methylimidazole, or omitted, indicating that the heterocycle plays a role in the mechanism of hydrolysis. Overall, the data compiled in Table 1 show the following trends: (i) hydrolysis is fastest when the first amino acid residue is proline, (ii) phosphoramidates of secondary amines hydrolyze faster than those of primary amines, (iii) amines without a carboxy function at the  $\alpha$ -position give more stable phosphoramidates. Also, (iv) the longer the peptide chain, the more resistant the phosphoramidate is to hydrolysis, and when the  $\alpha$ -functionality is an ester, the rate of hydrolysis drops. A cyclic structure, as in pyrrolidine, combined with the carboxylate at the  $\alpha$ -position (proline) appears to be the best structural arrangement to achieve rapid hydrolysis.

The kinetics of hydrolysis suggest that the structural properties of the amino acid residue in nucleosidic phosphoramidates are important for the release of the nucleotide. However, to the best of our knowledge no crystal structure of an unmodified aminoacyl-nucleoside phosphoramidate had been published to date. There are crystal structures of methyl esters of L- or D-alanyl or tryptophanyl phosphoramidates of purines complexed to the human Hint1 protein,<sup>[33]</sup> and a search of the Cambridge Structural Database gave structures of prodrug forms of phosphoramidates, that is, the phenyl ester form of phosphoramidates (Scheme 1), but no structures of the free aminoacyl nucleotides. Therefore, we undertook crystallization experiments with a series of aminoacyl phosphoramidates, including Gly-A, Pro-A,  $\beta$ Pro-A, Phe-A, and Arg-A. We tested conditions commonly employed for crystallization of nucleosides and nucleotides from aqueous solution, using slow evaporation of solvent and high or saturating concentrations of the target compound, either with or without the addition of precipitants, to gradually force the compound out of solution. We also used the hanging or sitting drop vapor diffusion techniques and mixtures of water with various amounts of methanol, ethanol, isopropanol, or acetonitrile, that had previously been used successfully for growing crystals of DNA and RNA mini-duplexes.<sup>[37]</sup> Ultimately, we only obtained crystals of Arg-A, but these were of insufficient quality for structure determination.

In view of the difficulties encountered, we considered an approach used successfully with chemically modified oligodeoxynucleotides that resisted crystallization, namely co-crystallization with a protein that acts as a scaffold. For the nucleosidic phosphoramidates, we settled on ribonuclease A (RNase A), an enzyme that may be the best-studied protein of the 20th century.<sup>[38]</sup> A large number of crystal structures of complexes between RNase A and mono- and dinucleotide inhibitors have been reported, for example, those of the endonuclease bound to 3',5'-ADP, 2',5'-ADP, 5'-ADP, U-2'-p and U-3'-p.<sup>[39]</sup> In most cases, crystals of complexes were obtained by soaking apo-form RNase A crystals in solutions of nucleotides.

All our attempts to co-crystallize RNase A with selected phosphoramidates, such as Gly-A and Pro-A, using 1 mM RNase A and between 1 and 5 mM concentrations of phosphoramidate met with failure. We then followed proto-

cols reported for crystal structures of RNase A complexes with 5'-AMP and 5'-IMP<sup>[40]</sup> or 5'-AMP and 3'-UMP<sup>[41]</sup> that relied on soaks of apo-form RNase A crystals in solutions of the nucleotides at concentrations between 50 and 200 mM, soaking RNase A crystals for up to 4 h (Pro-A) or as long as overnight (Gly-A). Crystals of the complexes with  $\beta$ Pro-A and Phe-A were obtained in a similar fashion. Soaks, data collection, phasing and preliminary refinement were typically repeated multiple times until inspection of the initial electron density revealed a well-defined phosphoramidate at least at one of the two RNase A active sites. Thus, we determined crystal structures of RNase A complexes with Gly-A, Pro-A,  $\beta$ Pro-A and Phe-A at resolutions of between 1.45 and 1.88 Å (Figure 3 and SI).

All crystals belonged to space group C2 with an asymmetric unit that contains two RNase A molecules. For some of the structures, only one of the two enzymes per asymmetric unit harbored a fully occupied aminoacyl phosphoramidate. The electron density present at the active site of the other RNase A molecule was typically limited to nucleobase and phosphate, consistent with a partially occupied ligand in those cases. Crystals of the complexes with Gly-A and Phe-A allowed refinement of complete phosphoramidates at both active sites. With Pro-A and  $\beta$ Pro-A crystals, one active site only showed electron density for AMP. In all structures, the aminoacyl-AMPs occupy the position of the 3'-nucleotide of the RNase A-catalyzed 3'-5'-phosphodiester cleavage reaction.<sup>[38]</sup> They display distinct orientations vis-à-vis the catalytic residues His-12, His-119 and Lys-41, and the amino acid contacted by the base of the 5'-nucleotide, Thr-45

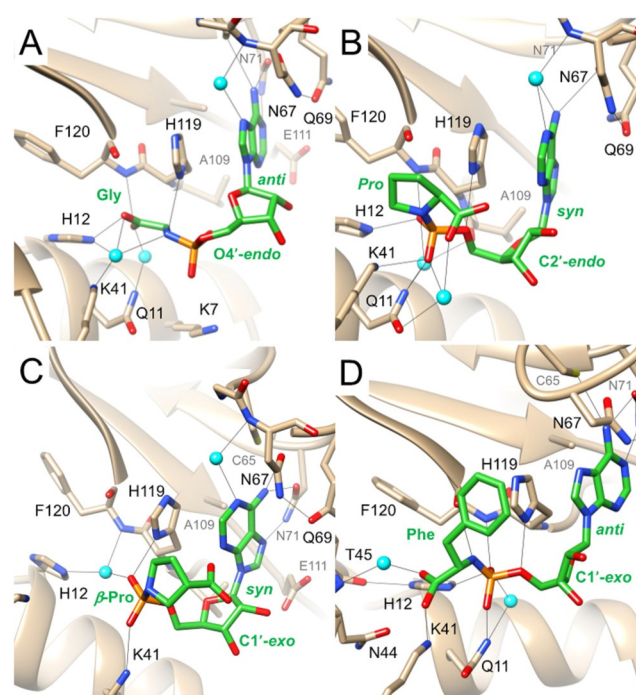


**Figure 3.** Crystal structures of RNase A-phosphoramidate complexes. Views of the active site with bound A) Gly-A, B) Pro-A, C)  $\beta$ Pro-A, and D) Phe-A. Glycosidic angles and sugar puckers are indicated, selected RNase A side chains are labeled, water molecules are cyan spheres, and H-bonds are drawn with thin solid lines.

(Figure 3). Their overall conformations also exhibit significant differences, particularly in terms of the relative orientations of amino acid side chain and adenine base (Figures 3), such as adenosine in Pro-A and  $\beta$ Pro-A adopting a *syn* conformation (Figures 3 B, C). The Phe-A phosphoramidates in the two independent complexes display almost identical conformations with the base in the *anti* orientation. Conversely, the conformations of the two independent Gly-A molecules are quite different, with adenine in the *syn* orientation in one (Figure 4 B) and in the *anti* orientation in the other (Figure 4 C).

In the four structures, we observed various distances between carboxylate oxygens (O) and the phosphorus of the phosphoramidate, as well as different O...P-O5' angles (Figures 3,4). The distance/angle pairs in the RNase A complexes are as follows, whereby bold font marks geometries with more closely spaced carboxylate oxygen and phosphorus atoms: Pro-A, **3.5 Å/87°** and **4.2 Å/63°** (Figure 4 A); Gly-A **3.4 Å/99°** and **4.6 Å/124°** (Figure 4 B); Gly-A **4.2 Å/109°** and **4.6 Å/115°** (Figure 4 C);  $\beta$ Pro-A, **4.1 Å/60°** and **5.0 Å/58°**; Phe-A (molecule A) **3.0 Å/158°** and **4.4 Å/126°**; and Phe-A (molecule B) **3.5 Å/150°** and **4.3 Å/127°**. Because the phosphoramidates adopt slightly different orientations vis-à-vis active site residues His-12, Lys-41 and His-119 in the individual structures (Figure 3), it is clear that the interactions with RNase A exert some influence on their conformations. Inspection of the electron densities of the complex structures did not indicate that RNase A is capable of cleaving the phosphoramidate moiety. However, we did not further analyze the contents of soaked crystals of RNase A by NMR or alternative approaches.

These caveats notwithstanding, carboxylate oxygen and P-O5' bond exhibit quite similar, adjacent orientations in Pro-A (Figure 4 A) and Gly-A (Figure 4 B, C). These produce close proximity between carboxylate oxygen and phosphorus that are required for formation of the five-membered ring, as proposed in the mechanistic picture shown in Figure 5 A. By comparison, the conformations observed for Phe-A show a carboxylate oxygen that is poised for attack at the phosphorus with subsequent in-line displacement of O5'. Apparently, this reaction does not take place under our conditions, as the main pathway is release of the amino

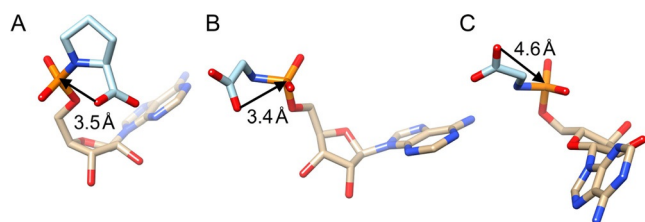


**Figure 4.** Conformations of A) Pro-A and B, C) Gly-A as observed in crystal structures of the respective complexes with RNase A. RNase A crystals contain two independent protein molecules and Gly-A bound to both could be resolved in the electron density maps. Conversely, in the structure of the complex with Pro-A bound to RNase A, only one complete Pro-AMP molecule could be visualized. Distances between phosphorus and the carboxylate oxygen that will „plausibly“ carry out the nucleophilic attack on the phosphate are indicated with an arrow.

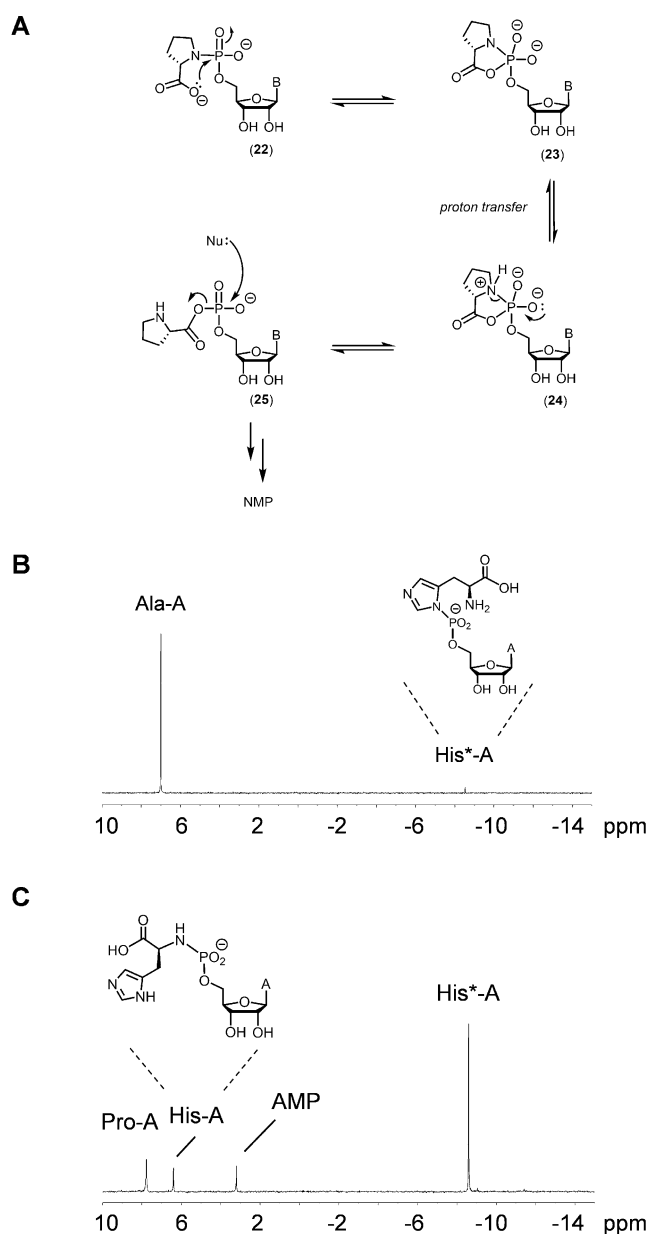


**Figure 5.** A) Proposed mechanism for the hydrolysis of prolinyl phosphoramidates; Nu, nucleophile. B)  $^{31}\text{P}$  NMR spectrum, assay with Ala-A and histidine after 1 d, C)  $^{31}\text{P}$  NMR spectrum, assay with Pro-A and histidine after 1 d. Conditions for B/C): 10 mM nucleotide, 0.15 M histidine, 0.5 M HEPES, 0.08 M  $\text{MgCl}_2$ , pH 7.5, 37°C.

substituent, not cleavage of the phosphoester bond to the nucleoside, a reaction that would be detrimental to the function of the prodrugs to release a monophosphate, which needs only two more phosphorylations to become the triphosphate substrate for the RdRp. In terms of the desired reactivity, proline with the basic secondary amino group and the preorganization provided by the pyrrolidine ring appears to be the most favorable structure.

The crystallographic evidence can be combined with other factors that may explain the rapid hydrolysis of proline NMPs at pH 7.5, such as the basicity of the nitrogen. Pyrrolidine ( $\text{p}K_a$  11.3) is slightly more basic than proline ( $\text{p}K_a$  10.6), most

probably compensating for the lack of the carboxy function of the latter that helps to liberate the amine, either by proton transfer or by driving reactivity through intramolecular attack (Figure 5A). The latter would lead to a rigid bicyclic intermediate in which the amine/ammonium group may find itself in an apical position more readily than for conformationally more flexible amino acids. When the *P*–*N* bond is cleaved, a labile mixed anhydride should result that undergoes rapid reaction with a nucleophile.

We note that the scenario of Figure 5A is different from the pathway for decomposition of nucleosidic phosphoramidates proposed by Herdewijn<sup>[29]</sup> or Lönnberg<sup>[42]</sup> for acyclic amino acids in hot aqueous solution, which involves hydrolysis of the *P*–*O* bond to liberate the nucleoside, not the nucleotide. The alternative attack on the phosphorus, to liberate the nucleotide from a mixed anhydride, had previously been proposed by Ricci et al. in a DFT study on ProTide prodrugs.<sup>[43]</sup> Because  $\beta$ -proline is most probably sterically incapable of forming the cyclic intermediate, the slow hydrolysis of  $\beta$ Pro-A supports this proposal. The much reduced nucleophilicity of the ester group in MeO-Pro-A and the amide group of peptido nucleotides can also be explained by the model involving the cyclic intermediates. A more remotely related finding, the rapid hydrolysis of the ester linkage connecting proline to the 3'-terminus of tRNA,<sup>[44]</sup> also points to readily occurring intramolecular attacks, facilitated by the rigid structure of the cyclic amino acid.

The mixed anhydride formed upon cleavage of the *P*–*N* bond (**25**) may react with a number of different nucleophiles. For reactions in 1-ethylimidazole-containing buffer, the *N3* of the heterocycle appears to be the dominant nucleophile, which then hydrolyzes to liberate the free nucleotide. This was revealed by a quantitative systems chemistry analysis<sup>[36]</sup> of the reaction of Pro-A (section 6 of the SI). The kinetics show a quick rise of the concentration of the imidazolium phosphate with a maximum at 1 h. If the free nucleotide had been released via nucleophilic attack on the carboxy side of the mixed anhydride, the imidazolium species would not have been observed, as quantitatively confirmed in fitting runs for either scenario, of which only the one involving attack on the phosphorus proved compatible with the experimental data.

This attack of an imidazole ring as the main path leading to hydrolysis is interesting, as it is analogous to what has been reported for hydrolysis mediated by Hint enzymes.<sup>[33]</sup> To confirm that the attack does not require the active site of an enzyme, we incubated Pro-A and Ala-A with the amino acid histidine in buffer devoid of 1-ethylimidazole. In either case, the imidazolides were found in the equilibrium (Figure 5B/C). For Pro-A, the formation of this species is much faster than for Ala-A, and its hydrolysis then leads to free AMP, with a reaction via the *N* $\alpha$ -amidate as a minor pathway. This data suggests that imidazolides formed with histidine components of the cell can induce the release of nucleoside 5'-monophosphates without the need for a Hint enzyme. Because the release pathway operates on the timescale of days, imidazolide intermediates may act as reservoirs that slowly liberate nucleoside monophosphates. This is relevant for nucleoside phosphate prodrugs, particularly when they are

to be employed in tissues that do not have high levels of enzymes with phosphoramidase activity.

## Conclusion

Remdesivir has been approved in Japan and has obtained emergency use authorization for treatment of COVID-19 in the US, but its effect on the mortality of COVID-19 is modest. The triphosphate form of this nucleoside is a good inhibitor of RdRp's of RNA viruses but achieving sufficiently high cellular concentrations of this triphosphate in the target tissues for a viral respiratory disease is a hurdle that may not be easy to overcome for a prodrug designed analogously to sofosbuvir, which acts on hepatocytes. Prodrugs with the ability to release the drug independent of phosphoramidase enzymes are therefore interesting alternatives. Our data shows that the release of nucleoside monophosphates from amino acid phosphoramidates of nucleosides in enzyme-free fashion is fast for proline. The effect was found for all three nucleobases tested (A, C and U), and modifications of the sugar or the glycosidic bond of yet to be synthesized remdesivir derivatives are unlikely to suppress it. Furthermore, we show that X-ray crystal structures of such reactive species can be obtained by soaking RNase A crystals with solutions of the phosphoramidates, and that the amino acid nucleotides are free to adopt different conformations in the complexes with the chaperone, including conformations where the carboxylate is poised to attack the phosphorus center. Overall, our results point to step-wise non-enzymatic hydrolysis as a pathway that can liberate nucleoside monophosphates at body temperature and pH 7.5, findings that are significant for prodrugs of polymerase inhibitors.

## Acknowledgements

We thank D. Pfeffer, D. Göhringer, M. Räuchle, and H. Griesser for sharing results and compounds, and Dr. E. Kervio for discussions. This work was supported by Volkswagen Foundation (grant Az 92 768) and Deutsche Forschungsgemeinschaft (DFG, German Research Foundation) project ID 364653263—TRR 235. Open access funding enabled and organized by Projekt DEAL.

## Conflict of interest

The authors declare no conflict of interest.

**Stichwörter:** antivirals · nucleotides · phosphoramidates · prodrugs · SARS-CoV-2

- [1] Y. Gao, L. Yan, Y. Huang, F. Liu, Y. Zhao, L. Cao, T. Wang, Q. Sun, Z. Ming, L. Zhang, J. Ge, L. Zheng, Y. Zhang, H. Wang, Y. Zhu, C. Zhu, T. Hu, T. Hua, B. Zhang, X. Yang, J. Li, H. Yang, Z. Liu, W. Xu, L. W. Guddat, Q. Wang, Z. Lou, Z. Rao, *Science* **2020**, 368, 779.
- [2] E. De Clercq, *Nat. Rev. Drug Discovery* **2007**, 6, 1001.

- [3] A. M. Shannon, N. T.-T. Le, B. Selisko, C. Eydoux, K. Alvarez, J.-C. Guillemot, E. Decroly, O. Peersen, F. Ferron, B. Canard, *Antiviral Res.* **2020**, *178*, 104793.
- [4] M. Slusarczyk, M. Serpi, F. Pertusati, *Antiviral Chem. Chemother.* **2018**, *26*, 1.
- [5] C. Meier, *Antiviral Chem. Chemother.* **2017**, *25*, 69.
- [6] C. McGuigan, R. N. Pathirana, N. Mahmood, K. G. Devine, A. J. Hay, *Antiviral Res.* **1992**, *17*, 311.
- [7] C. McGuigan, R. N. Pathirana, N. Mahmood, A. J. Hay, *Med. Chem. Lett.* **1992**, *2*, 701.
- [8] M. J. Sofia, D. Bao, W. Chang, J. Du, D. Nagarathnam, S. Rachakonda, P. G. Reddy, B. S. Ross, P. Wang, H.-R. Zhang, S. Bansal, C. Espiritu, M. Keilman, A. M. Lam, H. M. M. Steuer, C. Niu, M. J. Otto, P. A. Furman, *J. Med. Chem.* **2010**, *53*, 7202.
- [9] H. Chapman, M. Kernan, E. Prisbe, J. Rohloff, M. Sparacino, T. Terhorst, R. Yu, *Nucleosides Nucleotides Nucleic Acids* **2001**, *20*, 621.
- [10] R. T. Eastman, J. S. Roth, K. R. Brimacombe, A. Simeonov, M. Shen, S. Patnaik, M. D. Hall, *ACS Cent. Sci.* **2020**, *6*, 672.
- [11] W. C. Ko, J. M. Rolain, N. Y. Lee, P. L. Chen, C. T. Huang, P. I. Lee, P. R. Hsueh, *Int. J. Antimicrob. Agents* **2020**, *55*, 105933.
- [12] J. E. Tomassini, K. Getty, M. W. Stahlhut, S. Shim, B. Bhat, A. B. Eldrup, T. P. Prakash, S. S. Carroll, O. Flores, M. MacCoss, D. R. McMasters, G. Migliaccio, D. B. Olsen, *Antimicrob. Agents Chemother.* **2005**, *49*, 2050.
- [13] M. Derudas, D. Carta, A. Branciale, C. Vanpouille, A. Lisco, L. Margolis, J. Balzarini, C. McGuigan, *J. Med. Chem.* **2009**, *52*, 5520.
- [14] D. Siegel, H. C. Hui, E. Doerffler, M. O. Clarke, K. Chun, L. Zhang, S. Neville, E. Carra, W. Lew, B. Ross, Q. Wang, L. Wolfe, R. Jordan, V. Soloveva, J. Knox, J. Perry, M. Perron, K. M. Stray, O. Barauskas, J. Y. Feng, Y. Xu, G. Lee, A. L. Rheingold, A. S. Ray, R. Bannister, R. Strickley, S. Swaminathan, W. A. Lee, S. Bavari, T. Cihlar, M. K. Lo, T. K. Warren, R. L. Mackman, *J. Med. Chem.* **2017**, *60*, 1648.
- [15] T. K. Warren, R. Jordan, M. K. Lo, A. S. Ray, R. L. Mackman, V. Soloveva, D. Siegel, M. Perron, R. Bannister, H. C. Hui, N. Larson, R. Strickley, J. Wells, K. S. Stuthman, S. A. Van Tongeren, N. L. Garza, G. Donnelly, A. C. Shurtleff, C. J. Retterer, D. Gharaibeh, R. Zamani, T. Kenny, B. P. Eaton, E. Grimes, L. S. Welch, L. Gomba, C. L. Wilhelmsen, D. K. Nichols, J. E. Nuss, E. R. Nagle, J. R. Kugelman, G. Palacios, E. Doerffler, S. Neville, E. Carra, M. O. Clarke, L. Zhang, W. Lew, B. Ross, Q. Wang, K. Chun, L. Wolfe, D. Babusis, Y. Park, K. M. Stray, I. Trancheva, J. Y. Feng, O. Barauskas, Y. Xu, P. Wong, M. R. Braun, M. Flint, L. K. McMullan, S. S. Chen, R. Fearn, S. Swaminathan, D. L. Mayers, C. F. Spiropoulou, W. A. Lee, S. T. Nichol, T. Cihlar, S. Bavari, *Nature* **2016**, *531*, 381.
- [16] E. Procházková, R. Navrátil, Z. Janeba, J. Roithová, O. Baszczyński, *Org. Biomol. Chem.* **2019**, *17*, 315.
- [17] A. Krakowiak, H. C. Pace, G. M. Blackburn, M. Adams, A. Mekhalifa, R. Kaczmarek, J. Baraniak, W. J. Stec, C. Brenner, *J. Biol. Chem.* **2004**, *279*, 18711.
- [18] G. Liang, C. E. Webster, *Org. Biomol. Chem.* **2017**, *15*, 8661.
- [19] E. Murakami, T. Tolstykh, H. Bao, C. Niu, H. M. M. Steuer, D. Bao, W. Chang, C. Espiritu, S. Bansal, A. M. Lam, M. J. Otto, M. J. Sofia, P. A. Furman, *J. Biol. Chem.* **2010**, *285*, 34337.
- [20] P. A. Furman, E. Murakami, C. Niu, A. M. Lam, C. Espiritu, S. Bansal, H. Bao, T. Tolstykh, H. M. Steuer, M. Keilman, V. Zennou, N. Bourne, R. L. Veselenak, W. Chang, B. S. Ross, J. Du, M. J. Otto, M. J. Sofia, *Antiviral Res.* **2011**, *91*, 120.
- [21] E. Murakami, T. Wang, D. Babusis, E.-I. Lepist, D. Sauer, Y. Park, J. E. Vela, R. Shih, G. Birkus, D. Stefanidis, C. U. Kim, A. Cho, A. S. Ray, *Antimicrob. Agents Chemother.* **2014**, *58*, 1943.
- [22] D. Babusis, M. P. Curry, B. Kirby, Y. Park, E. Murakami, T. Wang, A. Mathias, N. Afdhal, J. G. McHutchison, A. S. Ray, *Antimicrob. Agents Chemother.* **2018**, *62*, e02587.
- [23] C. McGuigan, P. Murziani, M. Slusarczyk, B. Gonczy, J. V. Voorde, S. Liekens, J. Balzarini, *J. Med. Chem.* **2011**, *54*, 7247.
- [24] C. McGuigan, H. W. Tsang, P. W. Sutton, *Antiviral Chem. Chemother.* **1998**, *9*, 109.
- [25] D. Saboulard, L. Naesens, D. Cahard, A. Salgado, R. Pathirana, S. Velazquez, C. McGuigan, E. De Clercq, J. Balzarini, *Mol. Pharmacol.* **1999**, *56*, 693.
- [26] T.-F. Chou, J. Baraniak, R. Kaczmarek, X. Zhou, J. Cheng, B. Ghosh, C. R. Wagner, *Mol. Pharm.* **2007**, *4*, 208.
- [27] O. Adelfinskaya, P. Herdewijn, *Angew. Chem. Int. Ed.* **2007**, *46*, 4356; *Angew. Chem.* **2007**, *119*, 4434.
- [28] M. Maiti, M. Maiti, J. Rozenski, S. De Jonghe, P. Herdewijn, *Org. Biomol. Chem.* **2015**, *13*, 5158.
- [29] M. Maiti, S. Michielsens, N. Dyubankova, M. Maiti, E. Lescrinier, A. Ceulemans, P. Herdewijn, *Chem. Eur. J.* **2012**, *18*, 857.
- [30] B. Juodka, S. Sasnauskiene, Z. Shabarova, *J. Carbohydr. Nucleosides Nucleotides* **1981**, *8*, 519.
- [31] Z. A. Shabarova, *Bioorganicheskaya Khimiya* **1981**, *7*, 240.
- [32] D. P. Drontle, C. R. Wagner, *Mini-Rev. Med. Chem.* **2004**, *4*, 409.
- [33] K. M. Maize, R. Shah, A. Strom, S. Kumarapperuma, A. Zhou, C. R. Wagner, B. C. Finzel, *Mol. Pharm.* **2017**, *14*, 3987.
- [34] M. Jauker, H. Griesser, C. Richert, *Angew. Chem. Int. Ed.* **2015**, *54*, 14564; *Angew. Chem.* **2015**, *127*, 14772.
- [35] H. Griesser, P. Tremmel, E. Kervio, C. Pfeffer, U. E. Steiner, C. Richert, *Angew. Chem. Int. Ed.* **2017**, *56*, 1219; *Angew. Chem.* **2017**, *129*, 1239.
- [36] P. Tremmel, H. Griesser, U. E. Steiner, C. Richert, *Angew. Chem. Int. Ed.* **2019**, *58*, 13087; *Angew. Chem.* **2019**, *131*, 13221.
- [37] a) J. M. Rosenberg, N. C. Seeman, J. J. Park Kim, F. L. Suddath, H. B. Nicholas, A. Rich, *Nature* **1973**, *243*, 150; b) J. M. Rosenberg, N. C. Seeman, R. O. Day, A. Rich, *J. Mol. Biol.* **1976**, *69*, 979; c) M. Egli, R. Gessner, L. D. Williams, G. J. Quigley, G. A. van der Marel, J. H. van Boom, A. Rich, C. A. Frederick, *Proc. Natl. Acad. Sci. USA* **1990**, *87*, 3235; d) M. Egli, P. Lubini, M. Bolli, M. Dobler, C. Leumann, *J. Am. Chem. Soc.* **1993**, *115*, 5855.
- [38] R. T. Raines, *Chem. Rev.* **1998**, *98*, 1045.
- [39] D. D. Leonidas, G. B. Chavali, N. G. Oikonomakos, E. D. Chrysinia, M. N. Kosmopoulou, M. Vlasi, C. Frankling, K. R. Acharya, *Protein Sci.* **2003**, *12*, 2559.
- [40] G. N. Hatzopoulos, D. D. Leonidas, R. Kardakaris, J. Kobe, N. G. Oikonomakos, *FEBS J.* **2005**, *272*, 3988.
- [41] D. Gagné, R. L. French, C. Narayanan, M. Simonović, P. K. Agarwal, N. Doucet, *Structure* **2015**, *23*, 2256.
- [42] M. Ora, J. Ojanper, H. Lönnberg, *Chem. Eur. J.* **2007**, *13*, 8591.
- [43] A. Ricci, A. Branciale, *J. Comput. Chem.* **2012**, *33*, 1029.
- [44] J. R. Peacock, R. R. Walvoord, A. Y. Chang, M. C. Kozlowski, H. Gamper, Y. M. Hou, *RNA* **2014**, *20*, 758.

Manuskript erhalten: 19. Juni 2020

Veränderte Fassung erhalten: 4. August 2020

Akzeptierte Fassung online: 5. August 2020

Endgültige Fassung online: 15. September 2020